Nanoscale Advances

ROYAL SOCIETY OF CHEMISTRY

PAPER

View Article Online
View Journal | View Issue

Cite this: *Nanoscale Adv.*, 2022, **4**, 2339

Synergic effect of graphene oxide and boron nitride on the mechanical properties of polyimide composite films†

Yi Kai Cheng,[a] Benoît Denis Louis Campéon,[b] Seiji Obata[b] and Yuta Nishina *[ab]

Received 29th January 2022
Accepted 1st April 2022

DOI: 10.1039/d2na00078d

rsc.li/nanoscale-advances

The addition of two-dimensional (2D) materials into polymers can improve their mechanical properties. In particular, graphene oxide (GO) and hexagonal boron nitride (h-BN) are expected to be potential nanoplatelet additives for polymers. Interactions between such nanoplatelets and polymers are effective in improving the above properties. However, no report has investigated the effect of using two types of nanoplatelets that have good interaction with polymers. In this study, we fabricated polyimide (PI) films that contain two types of nanoplatelets, amine-functionalized h-BN (BN_{NH_2}) and GO. We have elucidated that the critical ratio and the content of BN_{NH_2} and GO within PI govern the films' mechanical properties. When the BN_{NH_2}/GO weight ratio was 52 : 1 and their content was 1 wt% in the PI film, the tensile modulus and tensile strength were increased by 155.2 MPa and 4.2 GPa compared with the pristine PI film.

Introduction

Polymer films with molecularly designed structures have been playing an important role in applications such as medical devices,[1] separators in batteries,[2–4] high-performance audio diaphragms,[5] and computer memory.[6] Therefore, the fabrication of polymers with targeted properties is of great interest for the development of next-generation technologies. Polymers have advantages such as their ease of processing, light weight, and chemical resistance compared with metallic materials.[7,8] Polyimide (PI), which was first synthesized in 1908,[9] has extremely high heat and chemical resistances, mechanical properties, and electrical insulation compared to other polymer materials. These properties enable PI to be used in a wide range of applications such as waterproof coatings,[10,11] speaker components,[12–14] separators for batteries,[15,16] gas separations,[17–19] and water purification membranes.[20,21]

The introduction of fillers has been investigated to improve the properties of polymer films. Addition of one- and/or two-dimensional (2D) carbon materials has been aimed at forming strong π–π interaction between the aromatic frameworks in PI and carbon materials.[22,23] For example, the physical properties of PI can be improved by the addition of low-dimensional carbon materials, such as carbon nanotubes,[24–26] graphene oxide (GO),[27–31] and amine-functionalized carbon materials.[32,33] Another promising filler with a honeycomb structure is hexagonal boron nitride (h-BN), which can interact strongly with 2D carbon materials.[34] Therefore, mixing with carbon composites of h-BN would exert a synergic effect, resulting in thermal conductivity, as well as thermoelectric and mechanical properties.[35–37] Several methods of modifying h-BN edges with hydroxyl groups or amino (NH_2) groups were reported recently.[38–40] However, the fabrication of the PI-BN/GO composite film and evaluation of its mechanical properties have not been reported so far.

In this study, we focused on edge functionalization of h-BN with NH_2 groups (BN_{NH_2}) to ensure a good affinity with GO and PI to improve mechanical strength. The BN_{NH_2} edge can bond with PI through amide bonds, while its basal plane retains a non-reactive honeycomb structure. Interestingly, h-BN and GO show good interaction with each other.[41–43] Therefore, we hypothesized that covering the basal plane of BN_{NH_2} with GO results in a filler with superior mechanical strength through interaction with PI at both the basal plane (oxy functional groups on GO) and edge (amino groups of BN_{NH_2}) of the 2D structure. In this context, we prepared a PI-BN_{NH_2}/GO composite containing both GO and BN_{NH_2} to elucidate the effect of employing multiple types of nanoplatelets in PI films (Fig. 1). As a result, the mechanical properties of PI films were improved by the introduction of BN_{NH_2}, and a further improvement was obtained with an additional small amount of GO.

Results and discussion

Synthesis and characterization of BN_{NH_2}

First, we synthesized amine-functionalized h-BN (BN_{NH_2}) by a ball milling method (details are given in the Experimental

[a]Graduate School of Natural Science and Technology, Okayama University, 3-1-1 Tsushima-naka Kita-ku, Okayama 700-8530, Japan. E-mail: nisina-y@cc.okayama-u.ac.jp

[b]Research Core for Interdisciplinary Sciences, Okayama University, 3-1-1 Tsushima-naka Kita-ku, Okayama 700-8530, Japan

† Electronic supplementary information (ESI) available. See https://doi.org/10.1039/d2na00078d

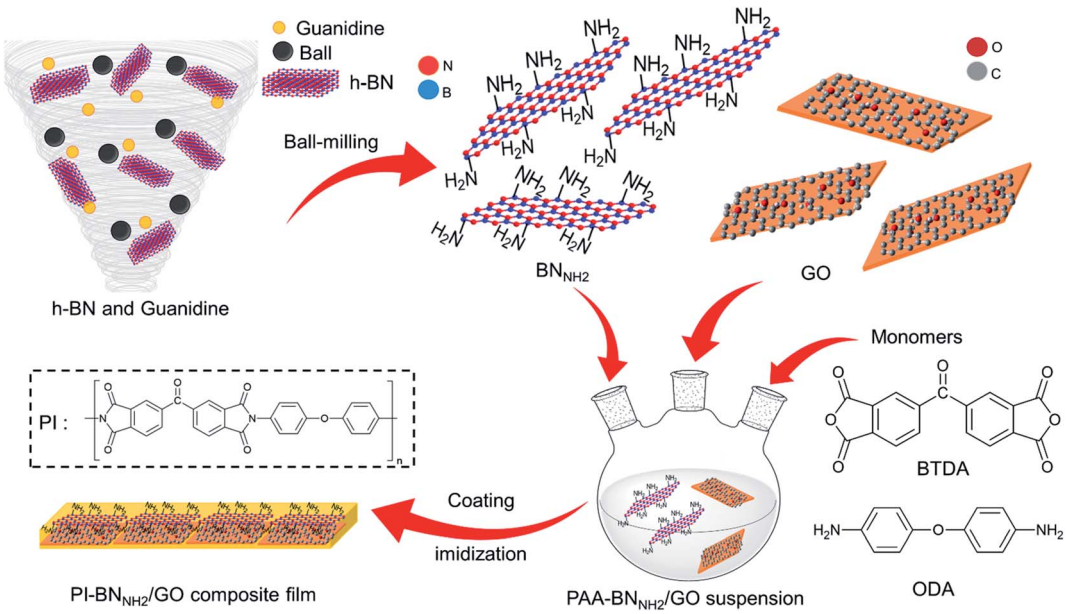

Fig. 1 Schematic illustration of the fabrication of the PI-BN_{NH_2}/GO composite film.

section). We used guanidine or urea as a nitrogen source. Hereafter, we call h-BN treated with urea BN_{NH_2}(U) and h-BN treated with guanidine BN_{NH_2}(G), respectively. After ball milling, dialysis was carried out to remove unreacted guanidine or urea. The specimens were treated by sonication for 1 h in dimethylacetamide (DMAc), resulting in a homogeneous dispersion (Fig. S1†).

The Fourier transform infrared (FTIR) spectra exhibited strong peaks at 780 cm^{-1} and 1380 cm^{-1} originating from the in-plane B–N stretching vibration and out-of-plane B–N–B bending vibration (Fig. S2†).[44,45] Furthermore, an additional peak appeared at around 3250 cm^{-1} in BN_{NH_2}(G). This peak is assigned to the N–H vibration mode.[46,47] Thermal gravimetric analysis (TGA) results are shown in Fig. 2a. According to the TGA results, BN_{NH_2}(U) and BN_{NH_2}(G) showed 2 wt% and 4 wt% loss, respectively, while pure h-BN did not show weight loss. These results indicate that functionalized h-BN was successfully synthesized and that more amine-functionalization proceeded with guanidine than with urea. Therefore, BN_{NH_2}(G) was used for the following experiments. X-ray diffraction (XRD) data are presented in Fig. 2b; BN_{NH_2}(G) showed two main characteristic diffraction peaks at 26.2° and 42.8° originating from the h-BN structure. Compared to the pristine h-BN, the (002) and (100) peak intensities of BN_{NH_2}(G) decreased. Thus, the FWHM of (002) was changed from 0.25 to 0.34; in contrast, the (002) peak position was not significantly shifted (Fig. S3†). These results suggest that h-BN sheets were exfoliated because of the physical force and/or the chemical functionalization during the ball milling process.

Reaction of BN_{NH_2} with an acid anhydride

To confirm the presence of NH_2 groups in BN_{NH_2}, we treated BN_{NH_2}(G) with 3,3′,4,4′-benzophenonetetracarboxylic dianhydride (BTDA) to form amide bonds. The detailed synthesis procedure is given in the Experimental section. TGA data of h-BN, BN_{NH_2}(G), and BN_{NH_2}(G) treated with BTDA (BN_{NH_2}(G)/BTDA) are presented

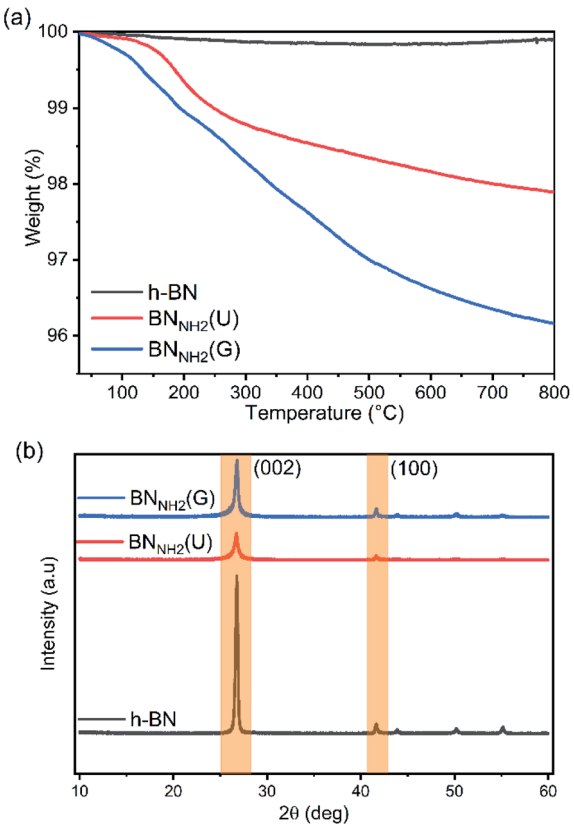

Fig. 2 (a) TGA curves of h-BN, BN_{NH_2}(U), and BN_{NH_2}(G) with a heating rate of 10 °C min^{-1}. (b) XRD patterns of BN_{NH_2}(G), BN_{NH_2}(U), and pristine h-BN.

in Fig. 3. For comparison, TGA data of h-BN treated with BTDA (h-BN/BTDA) are also presented in Fig. 3. The h-BN/BTDA sample showed two mass losses of 1.7 wt% and 2.2 wt% at 225 °C and 320 °C. On the other hand, the $BN_{NH_2}(G)$/BTDA sample showed two mass losses of 5.6 wt% and 4.2 wt% at 150 °C and 500 °C, respectively, corresponding to the release of water during the thermal imidization and the carbonization reactions.[48–50] After TGA analysis, only the surface of $BN_{NH_2}(G)$/BTDA turned black (Fig. 3b–e). Furthermore, FTIR spectra of $BN_{NH_2}(G)$/BTDA (Fig. S4a and b†) show an additional peak at 1720 cm^{-1} derived from the C═O vibration,[51,52] and the NH stretching vibration at 3520 cm^{-1} has slightly decreased (Fig. S4c†). The above description suggests that the NH_2 group on h-BN can bond with BTDA through an amide bond. In the case of h-BN/BTDA, C═O vibration at 1720 cm^{-1} was not observed (Fig. S4d†). The TGA and FTIR results confirm that NH_2 groups are present on h-BN, and the NH_2 groups can form amide bonds.

Fabrication of PI-$BN_{NH_2}(G)$ and PI-$BN_{NH_2}(G)$/GO composite films

DMAc is generally used as a solvent for the preparation of polyamic acid (PAA),[32,33] a precursor of PI. Therefore, the dispersibility of $BN_{NH_2}(G)$ and $BN_{NH_2}(G)$/GO was investigated in DMAc by sonication. The ratio of $BN_{NH_2}(G)$: GO was 10 : 1 and 100 : 1, and the obtained samples were termed $BN_{NH_2}(G)$/GO(10 : 1) and $BN_{NH_2}(G)$/GO(100 : 1), respectively. The suspensions were stable for more than one month at room temperature without visible precipitation (Fig. S1†). The particle size analysis (Fig. S5†) showed a mean size of 273 nm, 234 nm, and 223 nm for $BN_{NH_2}(G)$, $BN_{NH_2}(G)$/GO(100 : 1), and $BN_{NH_2}(G)$/GO(10 : 1), respectively.

Next, homogeneous suspensions of PAA composites were prepared in DMAc by a two-step process. Initially, sonication was employed to disperse $BN_{NH_2}(G)$ or $BN_{NH_2}(G)$/GO with 4,4′-diaminodiphenyl ether (ODA) and BTDA. Then, the as-obtained dispersion was mixed for 12 hours to allow the polymerization and formation of PAA composite suspensions, which are termed as PAA-$BN_{NH_2}(G)$, PAA-$BN_{NH_2}(G)$/GO(10 : 1), and PAA-$BN_{NH_2}(G)$/GO(100 : 1). These PAA composite suspensions were coated on glass and heated at 300 °C, resulting in PI composite films, termed as PI-$BN_{NH_2}(G)$, PI-$BN_{NH_2}(G)$/GO(10 : 1), and PI-$BN_{NH_2}(G)$/GO(100 : 1) (details are given in the Experimental section). A conventional method for the synthesis of PI films consists of heating PAA films at elevated temperatures within 200 to 300 °C.[53,54] The heating rate was kept as low as 5 °C min^{-1} to avoid the formation of bubbles within the PI film during the solvent evaporation.[55]

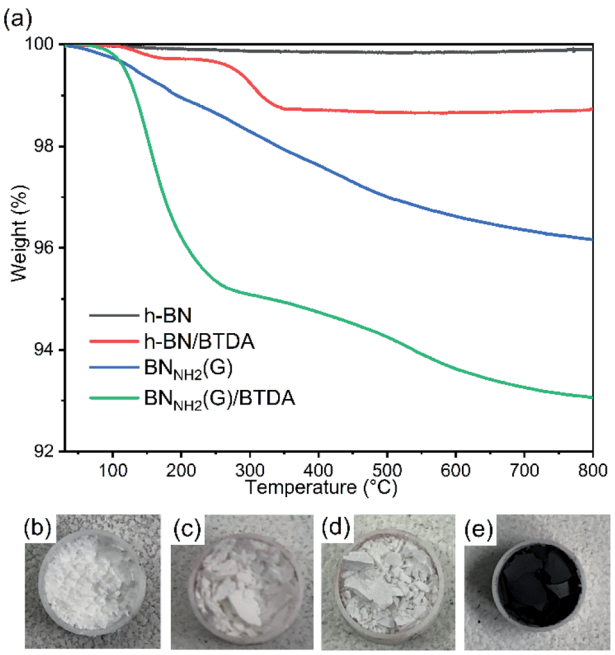

Fig. 3 (a) TGA curves of h-BN, h-BN/BTDA, $BN_{NH_2}(G)$, and $BN_{NH_2}(G)$/BTDA with a heating rate of 10 °C min^{-1} under a N_2 atmosphere. (b) h-BN after TGA. (c) h-BN/BTDA after TGA. (d) $BN_{NH_2}(G)$ after TGA. (e) $BN_{NH_2}(G)$/BTDA after TGA.

Mechanical properties of composite films

First, we investigated the effect of $BN_{NH_2}(G)$ and GO on PI film. According to Fig. 4 and Table 1, the tensile modulus of PI containing a low quantity (1 wt%) of GO showed a 22% increase over the tensile modulus of the pristine PI, although the tensile strength of the PI–GO was slightly decreased (Table 1, entries 1 and 2). The addition of only GO does not significantly improve the mechanical properties. A previous study also pointed out that GO decreased the tensile strength because the interaction between GO and PI is not strong.[31]

Next, we investigated the effect of the addition of h-BN, which improved the mechanical properties (Table 1, entry 3). Due to the surface roughness and wrinkles in h-BN (Fig. S6a and b†), the PI–hBN composite film has better mechanical properties than the pristine PI film, as reported previously.[56] Then, we investigated the composite with $BN_{NH_2}(G)$ to elucidate the effect of the functionalization. The tensile strength of PI containing a low quantity (0.5 wt%) of $BN_{NH_2}(G)$ showed a 23% increase over the tensile strength of the pristine PI (Table S1, entry 1†). Increasing the amount of $BN_{NH_2}(G)$ from 0.5 to 1 wt% improved the tensile strength by 44% (Table 1, entry 4). However, further increase of $BN_{NH_2}(G)$ to 3 wt% decreased both the tensile strength and tensile modulus (Table S1, entry 2†). These results indicate that an excess amount of $BN_{NH_2}(G)$ leads to reducing the positive effects of $BN_{NH_2}(G)$ in the PI matrix, probably caused by the stacking of $BN_{NH_2}(G)$ and void formation. Therefore, the optimal amount of $BN_{NH_2}(G)$ in PI is determined to be 1 wt%.

Finally, the combined use of GO and BN in the PI films was evaluated. The results demonstrated that PI films incorporating h-BN, $BN_{NH_2}(G)$ and GO showed superior mechanical properties than those with a single component (GO, h-BN, or $BN_{NH_2}(G)$) (Table 1, entries 2–6). This suggests that there is a good interaction between GO and BN, which enhances the mechanical properties of PI. According to Table 1 (entries 5 and 6), the tensile strength and tensile modulus of the $BN_{NH_2}(G)$/GO composite film are 22% and 23% higher than those of PI–

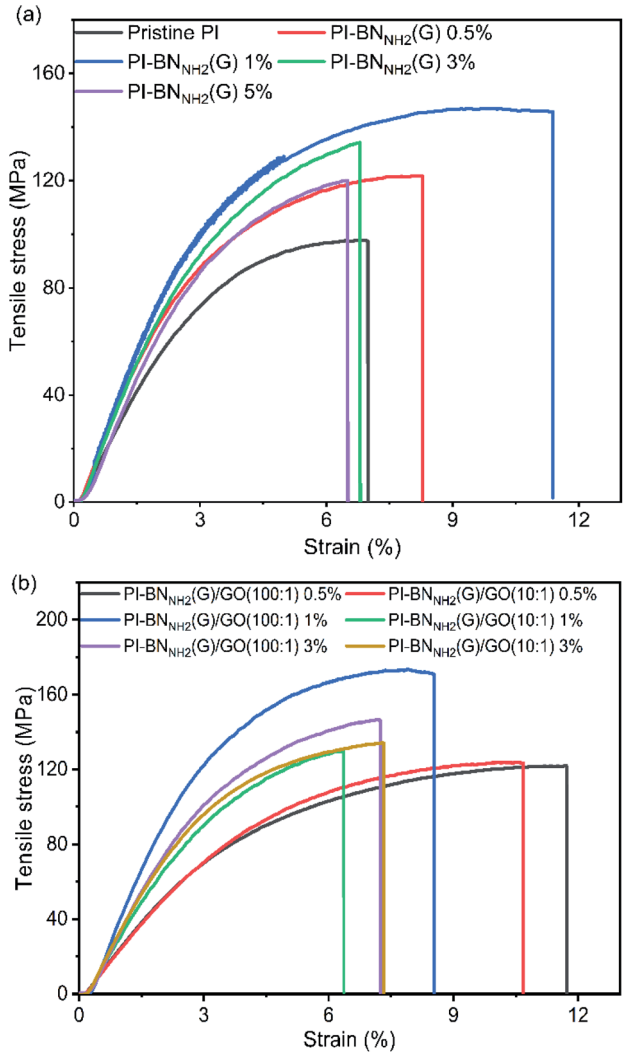

Fig. 4 (a) Stress–strain curves of the pristine PI film and PI-BN_{NH_2}(G) films. (b) Stress–strain curves of the PI-BN_{NH_2}(G) (100 : 1) and PI-BN_{NH_2}(G) (10 : 1) films.

hBN/GO. This proves that the edge-functionalization of h-BN improves the mechanical properties of the composite film. In addition, the PI-BN_{NH_2}(G)/GO composite film has a tensile strength of approximately 154.89 MPa, which is 65% higher than that of the original PI, and the tensile modulus was increased to 3.83 GPa, which is 69% higher than that of the original PI (Table 1, entry 1). Upon reducing the amount of BN_{NH_2}(G)/GO to 0.5 wt% BN_{NH_2}(G), the tensile strength and tensile modulus of PI were also reduced to 118.96 MPa and 2.84 GPa (Table S1, entry 4†). When the BN_{NH_2}(G)/GO ratio increased to 10 : 1, the tensile strength dropped to 137.33 MPa and the tensile modulus also dropped to 3.30 GPa (Table S1, entry 7†). Similar to only h-BN, there is a critical BN_{NH_2}(G)/GO amount for the improvement of the PI film's mechanical properties. Furthermore, these data also revealed that the ratio of BN_{NH_2}(G) to GO strongly affects the PI film's mechanical properties.

Based on our experimental results, we propose a model structure of PI-BN_{NH_2}(G)/GO. As reported previously, GO sheets are easily aggregated in the composite, resulting in lower tensile strength (Fig. S7a†).[31] In contrast, GO has a strong affinity with h-BN (Fig. S7c and d†).[41–43] The attachment of GO on the BN_{NH_2}(G) surface facilitates the interaction with PI because of the following synergic effect: (1) amide bond formation with BTDA at the edge of BN_{NH_2}(G),[57] and (2) amination of GO at the basal plane with ODA through an epoxy ring-opening reaction.[27] Due to these effects, the BN_{NH_2}(G)/GO composite would successfully enhance the mechanical properties of PI.

Ideally, BN_{NH_2}(G)/GO should be composed of single BN_{NH_2}(G) flakes covered by single-layer GO on both sides. According to AFM measurements, the average thickness of BN_{NH_2}(G) was 36 nm (Fig. S8†). Considering that the thickness of a single layer h-BN is 0.33 nm,[58] the prepared BN_{NH_2}(G) is composed of about 109 layers. As GO sheets are adsorbed only on the surface of BN_{NH_2}(G), the ideal ratio to fully cover the BN_{NH_2}(G) surface with GO is 109 layers of BN_{NH_2}(G) and 2 layers of GO. Considering the unit weight of BN and GO (the elemental ratio of C to O is 2 : 1), the ideal ratio of BN_{NH_2}(G)/GO is 52 : 1. To prove our speculation, we measured the mechanical properties of BN_{NH_2}(G)/GO that has a ratio of 52 : 1 (BN_{NH_2}(G)/GO(52 : 1)); its tensile modulus increased by 86%, and the tensile strength increased by 65% in comparison to the neat PI film (Table 1, entry 6). This specimen shows the highest tensile strength and tensile modulus among all specimens, which supports our hypothesis that surface coating of h-BN with GO is desirable for the strong interaction with PI.

Table 1 Mechanical properties of the neat PI film, PI-BN_{NH_2}(G) films, and PI-BN_{NH_2}(G)/GO films

Entry	Sample[a]	Tensile strength (MPa)	Tensile modulus (GPa)	Elongation at break (%)
1	Pristine PI	93.9 ± 3.4	2.2 ± 0.2	10.6 ± 3.6
2	PI–GO	90.2 ± 6.3	2.7 ± 0.1	4.4 ± 1.3
3	PI–hBN	110.9 ± 7.0	2.7 ± 0.1	6.8 ± 1.4
4	PI-BN_{NH_2}(G)	135.7 ± 5.4	3.1 ± 0.5	10.3 ± 1.7
5	PI–hBN/GO(100 : 1)	127.4 ± 6.8	3.1 ± 0.2	9.5 ± 3.1
6	PI-BN_{NH_2}(G)/GO(100 : 1)	154.8 ± 11.1	3.8 ± 0.4	7.8 ± 1.6
7	**PI-BN_{NH_2}(G)/GO(52 : 1)**	**155.2 ± 2.1**	**4.2 ± 0.1**	**7.1 ± 0.7**

[a] 1 wt% sample was used in the PI matrix.

Conclusions

In this research, we have demonstrated the improvement of the mechanical properties of PI films using a mixture of two types of materials, BN_{NH_2}(G) and GO. Improvement of the mechanical properties of composite films, including modulus, strength, and failure strain, has attracted tremendous interest in the field of materials science. Although the improvement of the modulus and/or strength has been realized in current studies,[59,60] the improvement of failure strain along with modulus and strength is rare in previous studies. Changing the ratio of BN and GO and their ratio to PI, we elucidated that there is a critical value at which the PI composite film showed the highest tensile modulus, tensile strength, and failure strain at the same time. This enhances the toughness and potential application of PI.

In the case of 1 wt% PI-BN_{NH_2}(G)/GO(52 : 1) composite film, the tensile modulus increased by 86%, and the tensile strength increased by 65% in comparison to the neat PI film. According to our results, we proposed and experimentally confirmed a model for the improvement of PI mechanical properties *via* the addition of BN_{NH_2}(G) and GO. In the case of BN_{NH_2}(G), only NH_2 groups at the edges interact with the raw materials of PI because the BN_{NH_2}(G) surface is inert. On the other hand, covering the BN_{NH_2}(G) surface with GO creates additional interaction between the BN_{NH_2}(G)/GO surface and the raw material of PI. Therefore, PI has a good affinity with it on the surfaces and edges, which enhances the mechanical properties of the PI composite film. In contrast, the excess amount of GO that is not attached to the h-BN surface causes the mechanical properties of the composite to deteriorate. Our results and the proposed mechanism will be useful guidelines for fabricating 2D composite materials in polymer matrixes.

Experimental section

Materials

Hexagonal boron nitride (h-BN) (average size 1–2 μm) was purchased from Showa Denko K.K., Japan. Guanidine hydrochloride (purity 99.0+%), 3,3′,4,4′-benzophenonetetracarboxylic dianhydride (BTDA, purity 96.0+%), 4,4′-diaminodiphenyl ether (ODA, purity 99.0+%), dimethylacetamide (DMAc, purity 98.0+%), sulfuric acid (H_2SO_4, purity 95.0+%), and potassium permanganate ($KMnO_4$, purity 99.3+%) were purchased from FUJIFILM Wako Pure Chemical Corporation, Japan.

Characterization instruments

The particle size analyzer (PSA) used in this work was ELSZ-2000N (Photal Otsuka Electronics, Japan). The samples for the PSA were dispersed in DMAc. Fourier transform infrared spectroscopy (FTIR) spectra of the samples were recorded between 400 and 4000 cm^{-1} with an IRTracer-100 (Shimadzu Corporation, Japan). Scanning electron microscope (SEM) measurements were performed with an S-5200 (Hitachi Limited, Japan) with an accelerating voltage of 30 kV. X-ray diffraction (XRD) measurements were performed on an AERIS equipped with single crystalline silicon (Panalytical, Netherlands). Thermal gravimetric analyses (TGA) were performed with a DTG-60AH (Shimadzu Corporation, Japan) from room temperature to 800 °C in nitrogen (N_2) at a heating rate of 10 °C min^{-1}. To measure the tensile strength of PI films, sample sheets were cut into 10 mm × 60 mm and were tested using an AG-Xplus Universal Testing Machine (Shimadzu, Japan) at a tensile testing rate of 1 mm min^{-1}.

Preparation of graphene oxide (GO)

GO was prepared using a modified Hummers method.[61,62] Graphite (3.0 g) was stirred in 95% H_2SO_4 (75 mL). $KMnO_4$ (9.0 g) was gradually added to the solution while keeping the temperature below 10 °C using an ice bath. The mixture was then stirred at 35 °C for 2 h. The resulting mixture was diluted with water (75 mL) under vigorous stirring and cooling so that the temperature did not exceed 50 °C. The suspension was further treated with 30% aq. H_2O_2 (7.5 mL). The resulting graphite oxide suspension was purified by centrifugation with water until neutralization, and freeze-dried.

Preparation of amine-functionalized hexagonal boron nitride (BN_{NH_2}(G))

BN_{NH2}(G) was prepared using a Pulverisette 7 Classic Line ball mill (Fritsch, Germany).[39,40] h-BN (0.5 g) and guanidine hydrochloride (10 g) were mixed using a ball mill at a rotation speed of 750 rpm for 16 h at ambient temperature. Water (*ca.* 50 mL) was added to the solid product. The resulting BN_{NH2}(G) suspension was purified by dialysis (membrane cutoff: 12 000–14 000 Da) in deionized (DI) water for 24 h (DI water was changed every 3 h, which was repeated 3 times, then left to stand for 16 h) to remove the guanidine hydrochloride. A 1 week dialysis treatment was also investigated (Fig. S9†), but no difference was detected from the 24 h treated sample. Therefore, the 24 h dialysis treatment was selected. Finally, the sample was ultrasonicated for 10 min in DI water, and freeze-dried.

Preparation of PI-BN_{NH_2}(G) composite films

To prepare PAA-BN_{NH_2}(G) suspensions of different concentrations, BN_{NH_2}(G) (0.026 g, 0.053 g, 0.161 g, or 0.274 g) was dispersed in DMAc (20 mL) by sonication for 1 h. ODA (2.0 g, 10 mmol) was added to the BN_{NH_2}(G) suspension by sonication for 10 min. Then, BTDA (3.2 g, 10 mmol) was added into the suspension, sonicated for 10 min, and cooled in a freezer at about −18 °C for 12 h.

A viscous PAA-BN_{NH2}(G) suspension was coated on glass using an MSK-AFA-III coater (MTI Corporation, USA) with a coating rate of 20 mm s^{-1}. The coating was heated at 90 °C for 1 h (heating speed 1 °C min^{-1} under nitrogen) to evaporate the solvent. Finally, PI was formed by heat-treatment from room temperature to 300 °C for 1 h (room temperature to 300 °C for 5 h under nitrogen).

Preparation of PI-BN_{NH_2}(G)/GO composite films

BN_{NH_2}(G)/GO(100 : 1) or BN_{NH_2}(G)/GO(10 : 1) (5.2 g) was dispersed in DMAc (20 mL) with sonication for 1 h. ODA (2.0 g, 10 mmol) was added to the BN_{NH_2}(G)/GO suspension with sonication for 10 min. BTDA (3.2 g, 10 mmol) was then added into the suspension and sonicated for 10 min, furnishing a PAA-BN_{NH_2}(G)/GO suspension. The mixture was coated on glass and heated at 90 °C for 1 h (heating speed: 1 °C min^{-1} under nitrogen) to evaporate the solvent. Next, heat-treatment was performed from room temperature to 300 °C over 5 h under a nitrogen atmosphere, followed by keeping at 300 °C for 1 h. PI-BN_{NH_2}(G)/GO composite films containing 0.5 wt%, 1 wt%, and 3 wt% BN_{NH_2}(G)/GO were prepared following the same procedures.

Conflicts of interest

There are no conflicts to declare.

Acknowledgements

Professor Mitsuhiro Okayasu is acknowledged for the mechanical properties measurements.

Notes and references

1 M. E. Alf, A. Asatekin, M. C. Barr, S. H. Baxamusa, H. Chelawat, G. Ozaydin-lnce, C. D. Petruczok, R. Sreenivasan, W. E. Tenhaeff, N. J. Trujillo, S. Vaddiraju, J. Xu and K. K. Gleason, *Adv. Mater.*, 2010, **22**, 1993–2027.
2 C. Wang, W. Zheng, Z. Yue, C. O. Too and G. G. Wallace, *Adv. Mater.*, 2011, **23**, 3580–3584.
3 Z. Chen, P. C. Hsu, J. Lopez, Y. Li, J. W. F. To, N. Liu, C. Wang, S. C. Andrews, J. Liu, Y. Cui and Z. Bao, *Nat. Energy*, 2016, **1**, 15009.
4 J. K. Kim, J. Scheers, J. H. Ahn, P. Johansson, A. Matic and P. Jacobsson, *J. Mater. Chem. A*, 2013, **1**, 2426–2430.
5 S. Kang, S. Cho, R. Shanker, H. Lee, J. Park, D. S. Um, Y. Lee and H. Ko, *Sci. Adv.*, 2018, **4**, 1–12.
6 Y. J. Park, I. S. Bae, S. Ju Kang, J. Chang and C. Park, *IEEE Trans. Dielectr. Electr. Insul.*, 2010, **17**, 1135–1163.
7 D. A. Bernards and T. A. Desai, *Soft Matter*, 2010, **6**, 1621–1631.
8 W. Ogieglo, H. Wormeester, K. J. Eichhorn, M. Wessling and N. E. Benes, *Prog. Polym. Sci.*, 2015, **42**, 42–78.
9 M. T. Bogert and R. R. Renshaw, *J. Am. Chem. Soc.*, 1908, **30**, 1135–1144.
10 Y. Ma, L. Xu, Z. He, J. Xie, L. Shi, M. Zhang, W. Zhang and W. Cui, *J. Mater. Chem. C*, 2019, **7**, 7360–7370.
11 T. Komamura, K. Okuhara, S. Horiuchi, Y. Nabae and T. Hayakawa, *ACS Appl. Polym. Mater.*, 2019, **1**, 1209–1219.
12 N. Hosoya, S. Baba and S. Maeda, *J. Acoust. Soc. Am.*, 2015, **138**, EL424–EL428.
13 K. M. Kim and K. Park, *J. Mech. Sci. Technol.*, 2013, **27**, 2923–2928.
14 M. Sharifzadeh Mirshekarloo, C. Y. Tan, X. Yu, L. Zhang, S. Chen, K. Yao, F. Cui, S. M. Pandit, S. H. Chong and S. T. Tan, *Appl. Acoust.*, 2018, **137**, 90–97.
15 H. G. Wang, S. Yuan, D. L. Ma, X. L. Huang, F. L. Meng and X. B. Zhang, *Adv. Energy Mater.*, 2014, **4**, 1–7.
16 Y. E. Miao, G. N. Zhu, H. Hou, Y. Y. Xia and T. Liu, *J. Power Sources*, 2013, **226**, 82–86.
17 T. H. Kim, W. J. Koros, G. R. Husk and K. C. O'Brien, *J. Membr. Sci.*, 1988, **37**, 45–62.
18 M. R. Coleman and W. J. Koros, *J. Membr. Sci.*, 1990, **50**, 285–297.
19 Y. Wang, Z. Low, S. Kim, H. Zhang, X. Chen, J. Hou, J. G. Seong, Y. M. Lee, G. P. Simon, C. H. J. Davies and H. Wang, *Angew. Chem.*, 2018, **130**, 16288–16293.
20 G. Q. Chen, C. A. Scholes, G. G. Qiao and S. E. Kentish, *J. Membr. Sci.*, 2011, **379**, 479–487.
21 M. Minelli, G. Cocchi, L. Ansaloni, M. G. Baschetti, M. G. De Angelis and F. Doghieri, *Ind. Eng. Chem. Res.*, 2013, **52**, 8936–8945.
22 M. Okamoto, T. Fujigaya and N. Nakashima, *Adv. Funct. Mater.*, 2008, **18**, 1776–1782.
23 S. Qin, C. Chen, M. Cui, A. Zhang, H. Zhao and L. Wang, *RSC Adv.*, 2017, **7**, 3003–3011.
24 M. Lebrón-Colón, M. A. Meador, J. R. Gaier, F. Solá, D. A. Scheiman and L. S. McCorkle, *ACS Appl. Mater. Interfaces*, 2010, **2**, 669–676.
25 C. Cui, W. Qian, M. Zhao, F. Ding, X. Jia and F. Wei, *Carbon*, 2013, **60**, 102–108.
26 W. Ning, Z. Wang, P. Liu, D. Zhou, S. Yang, J. Wang, Q. Li, S. Fan and K. Jiang, *Carbon*, 2018, **139**, 1136–1143.
27 D. Chen, H. Zhu and T. Liu, *ACS Appl. Mater. Interfaces*, 2010, **2**, 3702–3708.
28 N. D. Luong, U. Hippi, J. T. Korhonen, A. J. Soininen, J. Ruokolainen, L. S. Johansson, J. Do Nam, L. H. Sinh and J. Seppälä, *Polymer*, 2011, **52**, 5237–5242.
29 J. Y. Kong, M. C. Choi, G. Y. Kim, J. J. Park, M. Selvaraj, M. Han and C. S. Ha, *Eur. Polym. J.*, 2012, **48**, 1394–1405.
30 K. Kim, K. H. Nam, J. Lee, H. J. Kim, M. Goh, B. C. Ku and N. H. You, *Carbon*, 2017, **122**, 614–621.
31 Z. Chen, F. Tong, D. Zhu, X. Lu and Q. Lu, *ACS Appl. Polym. Mater.*, 2019, **1**, 914–923.
32 W. H. Liao, S. Y. Yang, J. Y. Wang, H. W. Tien, S. T. Hsiao, Y. S. Wang, S. M. Li, C. C. M. Ma and Y. F. Wu, *ACS Appl. Mater. Interfaces*, 2013, **5**, 869–877.
33 J. Y. Wang, S. Y. Yang, Y. L. Huang, H. W. Tien, W. K. Chin and C. C. M. Ma, *J. Mater. Chem.*, 2011, **21**, 13569–13575.
34 T. Chu, D. Liu, Y. Tian, Y. Li, W. Liu, G. Li, Z. Song, Z. Jian and X. Cai, *ACS Appl. Nano Mater.*, 2020, **3**, 5327–5334.
35 H. Li, R. Y. Tay, S. H. Tsang, W. Liu and E. H. T. Teo, *Electrochim. Acta*, 2015, **166**, 197–205.
36 H. Li, L. Jing, R. Y. Tay, S. H. Tsang, J. Lin, M. Zhu, F. N. Leong and E. H. T. Teo, *Chem. Eng. J.*, 2017, **328**, 825–833.
37 G. Yang, L. Zhao, C. Shen, Z. Mao, H. Xu, X. Feng, B. Wang and X. Sui, *Sol. Energy Mater. Sol. Cells*, 2020, **209**, 110441.
38 J. Wang, D. Liu, Q. Li, C. Chen, Z. Chen, P. Song, J. Hao, Y. Li, S. Fakhrhoseini, M. Naebe, X. Wang and W. Lei, *ACS Nano*, 2019, **13**, 7860–7870.

39 W. Lei, V. N. Mochalin, D. Liu, S. Qin, Y. Gogotsi and Y. Chen, *Nat. Commun.*, 2015, **6**, 8849.
40 C. Chen, J. Wang, D. Liu, C. Yang, Y. Liu, R. S. Ruoff and W. Lei, *Nat. Commun.*, 2018, **9**, 1902.
41 T. Huang, X. Zeng, Y. Yao, R. Sun, F. Meng, J. Xu and C. Wong, *RSC Adv.*, 2016, **6**, 35847–35854.
42 S. Byun, J. H. Kim, S. H. Song, M. Lee, J. J. Park, G. Lee, S. H. Hong and D. Lee, *Chem. Mater.*, 2016, **28**, 7750–7756.
43 X. He and Y. Wang, *Ind. Eng. Chem. Res.*, 2020, **59**, 1925–1933.
44 Y. Lin, T. V. Williams, T. B. Xu, W. Cao, H. E. Elsayed-Ali and J. W. Connell, *J. Phys. Chem. C*, 2011, **115**, 2679–2685.
45 Q. Weng, B. Wang, X. Wang, N. Hanagata, X. Li, D. Liu, X. Wang, X. Jiang, Y. Bando and D. Golberg, *ACS Nano*, 2014, **8**, 6123–6130.
46 R. Geick, C. H. Perry and G. Rupprecht, *Phys. Rev.*, 1966, **146**, 543–547.
47 Y. Shi, C. Hamsen, X. Jia, K. K. Kim, A. Reina, M. Hofmann, A. L. Hsu, K. Zhang, H. Li, Z. Y. Juang, M. S. Dresselhaus, L. J. Li and J. Kong, *Nano Lett.*, 2010, **10**, 4134–4139.
48 J. H. Chang and K. M. Park, *Eur. Polym. J.*, 2000, **36**, 2185–2191.
49 D. J. Liaw, K. L. Wang, Y. C. Huang, K. R. Lee, J. Y. Lai and C. S. Ha, *Prog. Polym. Sci.*, 2012, **37**, 907–974.
50 A. Mochizuki, T. Teranishi and M. Ueda, *Polym. J.*, 1994, **26**, 315–323.
51 S. Shin, J. Jang, S. H. Yoon and I. Mochida, *Carbon*, 1997, **35**, 1739–1743.
52 O. Gershevitz and C. N. Sukenik, *J. Am. Chem. Soc.*, 2004, **126**, 482–483.
53 A. Henglein, *Chem. Rev.*, 1989, **89**, 1861–1873.
54 M.-J. Brekner and C. Feger, *J. Polym. Sci., Part A: Polym. Chem.*, 1987, **25**, 2479–2491.
55 J. M. Lavin, D. M. Keicher, S. R. Whetten, P. B. Moore and S. S. Mani, *Solid Freeform Fabr.*, 2016, **2016**, 729–737.
56 C. Zhi, Y. Bando, C. Tang, H. Kuwahara and D. Golberg, *Adv. Mater.*, 2009, **21**, 2889–2893.
57 X. Zheng, J. Liu, K. Wang, R. Liu, Y. Yuan and X. Liu, *Prog. Org. Coat.*, 2018, **124**, 122–128.
58 M. Topsakal, E. Aktürk and S. Ciraci, *Phys. Rev. B: Condens. Matter Mater. Phys.*, 2009, **79**, 115442.
59 L. Chen, S. Chai, K. Liu, N. Ning, J. Gao, Q. Liu, F. Chen and Q. Fu, *ACS Appl. Mater. Interfaces*, 2012, **4**, 4398–4404.
60 C. Rodrigues, J. M. M. de Mello, F. Dalcanton, D. L. P. Macuvele, N. Padoin, M. A. Fiori, C. Soares and H. G. Riella, *J. Polym. Environ.*, 2020, **28**, 1216–1236.
61 W. S. Hummers and R. E. Offeman, *J. Am. Chem. Soc.*, 1958, **80**, 1339.
62 N. Morimoto, H. Suzuki, Y. Takeuchi, S. Kawaguchi, M. Kunisu, C. W. Bielawski and Y. Nishina, *Chem. Mater.*, 2017, **29**, 2150–2156.